53-39
47971

N95-32426

CHARACTERIZING THE FRAGMENTATION RING ON WITNESS PLATES

Final Report
NASA/ASEE Summer Faculty Fellowship Program -- 1994
Johnson Space Center

Prepared By:	Yuan-Liang A. Chen, Ph.D.,
Academic Rank:	Associate Professor,
College and Department:	Oklahoma Baptist University Division of Natural Science Shawnee, Ok 74081
NASA/JSC	
Directorate:	Space and Life Sciences
Division:	Solar System Exploration Division
Branch:	Planetary Sciences, SN 4
JSC Colleague:	Friedrich Horz
Date Submitted:	August 5, 1994

ABSTRACT

Hole-saw ring patterns on the witness plate are studied systematically. Aluminium alloy 1100 and 6061, inconel, teflon, and lead of different thickness were utilized for target material. The ring pattern are observed at D_p/T=1.98 to 4.02 for aluminium 1100 target, at D_p/T=1.55 to 10.51 for aluminium 6061 target, at D_p/T=4.41 to 9.98 for inconel target, at D_p/T=1.33 to 3.94 for teflon target, and at D_p/T=12.5 to 20.89 for lead target. The ring diameter showed a decreasing trend when D_p/T ratio increased. A analytical model is introduced. The crater distributions on the ring were investigated. The majority of the craters are in the neighborhood of 1100 μm to 1400 μm size. Many broken string like craters were observed on the ring as well as inside the ring.

INTRODUCTION

Impact experiments have been performed with a 5 mm Light Gas Gun (LGG) at the Experimental Impact Laboratory of the Solar System Exploration Division, SN4, with the objective to learn about the collisional fragmentation, dispersion and deceleration of hypervelocity projectiles as they pass through targets of variable thickness. Such experiments are of basic nature, yet they relate directly to the design of cosmic dust flight instruments and to the protection of space craft in near Earth orbit.

Consistent with the SN-interests in cosmic dust instruments, soda lime glass projectiles of variable diameters (50, 150, 1000, 3175 μm diameter) were accelerated in the LGG to some 6 km/s and they impacted and penetrated targets of various material and thickness. This project studied aluminum alloys (1100, 6061), teflon, inconel and lead targets. A so-called "witness plate" (aluminum or coper) was positioned behind these targets to intercept the entire debris cloud that exits penetrated targets; the fragments composing this cloud are of high speed and caused a complex pattern of secondary impacts on the witness plate. The geometry of these secondary crater patterns is the subject of this study. Specially, as target thickness approaches that of projectile diameter, a characteristic distinct ring of fragment-impacts is observed on the witness plate that contrasts markedly with irregular fragment dispersions at more massive target, and with distinctly radial deposits resulting from the penetration of thinner targets. The ring pattern was introduced with the descriptive term "**Hole-Saw Ring**" by F. Horz et al. (1) and were reported by Stilp et al.(2) , Pietkutowsky (3) and others for various projectile and target combinations and impact velocities. Many theoretical models (4,5) study the fragmentation of spheres and associated debris cloud. They suggest that the outer shell of projectile yields smaller and faster fragments while the more massive and slowfragments are due to the core of the projectile. At the time of this project being performed, there is no theory or model that derived these uniform fragment sizes and dispersion angles from the hole-saw ring. This distinct hole-saw ring occurs over a very limited range of D_p/T conditions. It appears to be an excellent boundary condition to test theoretical and computational models on collisional disruption of spherical objects.

The Project is divided into two parts: Phase I--Extract the necessary data from the witness-plates, such as the radius of the ring; the number and the size distribution of the craters in relation to the impact conditions. Study the physics rules that govern these phenomena. Phase II-- Use a hydrocode (CTH) to model the rings and establish a reliable tool to further investigate this special fragmentation case. During the ASEE/NASA summer program, we concentrated on the first part of the Project. The results from the Phase I will be utilized to continue Phase II of this project.

HOLE-SAW RING DIAMETERS ON THE WITNESS PLATE

This project intends to contribute to an improved understanding of hole-saw ring pattern on the witness plate. We investigated the witness plates due to various diameter soda-lime glass sphere projectiles impacted on different target materials. The projectile's diameter and target thickness ratios, D_p/T, were altered while the impact velocity was kept a constant. Four sizes of glass spheres were accelerated to 2 km/s - 6 km/s using the 5 mm LGG at the Experimental Impact Laboratory of the SSED, SN4. The 3.175 mm soda-lime glass sphere was selected for the purpose of a more uniform projectile material and better production of the hole-saw ring. We employed aluminum alloy 6061-T6 with thickness of 4.064 mm, 5.334 mm, 6.35 mm, 8.128 mm, 10.016 mm, and 16.002 mm as the target. The copper witness plate with various stand-off distance "L" was utilized to collect the information for analysis.

An Analytical Model

A debris-cloud model by J. Lawrence(6) is employed to study the relationship between the hole-saw ring diameter and the ratio of D_p/T.

The nondimensional mass ratio, M, is defined as

$$M = \frac{3\beta^2 \rho_t T}{2\rho_p D_p} = \frac{m_t}{m_p}, \qquad (1)$$

where the β is the ratio of the hole diameter to the projectile diameter, ρ_p is the density of the projectile, ρ_t is the density of target, T stands for the thickness of the target, m_t is the mass removed from the target, and m_p is the mass of the projectile.

A nondimensionalized impact velocity, V_p, is also defined as

$$V_p = \frac{u_p^2}{2\xi_b}. \qquad (2)$$

where is actually a nondimensional kinetic energy, ξ_b is considered an average energy per unit mass needed to break up or vaporize the materials involved in the penetration process. This term is integrated over the space and time involved in the pentration and debris generation process.

The half angle of the debris expansion, θ, is determined from $\theta = \sin^{-1}(u_e/u_c)$, where u_e is the debris expansion velocity, and u_c is the debris cloud center-of-mass velocity. The half angle of the debris expansion, θ, can also be written as

$$\theta = \sin^{-1}\left(M - \frac{(1+M)^2}{V_p} \right)^{1/2} . \qquad (3)$$

The hole-saw ring diameter, D, can be calculated by

$$D = 2\,L \tan\theta . \qquad (4)$$

Combine Eq.(3) and (4), the ring diameter is

$$D = 2\,L \left(\frac{V_p M - (1+M)^2}{V_p - V_p M + (1+M)^2} \right)^{1/2} . \qquad (5)$$

Replace the constants in the Eq.(1) by κ, and rewite it in the form

$$M = \frac{3}{2}\frac{\rho_t}{\rho_p}\left(\frac{D_h}{D_p}\right)^2\left(\frac{T}{D_p}\right) = \kappa\left(\frac{D_h}{D_p}\right)^2\left(\frac{T}{D_p}\right) = \kappa X , \qquad (6)$$

and substitute this equation into Eq.(5) to obtain

$$D = 2\,L \left(\frac{-\kappa^2 X^2 - (2+V_p)\kappa X - 1}{(2+V_p)\kappa^2 X^2 - (2-V_p)\kappa X + 1} \right)^{1/2} , \qquad (7)$$

a constant V_p for the fixed impact velocity and projectile/target material and thickness. Eq.(7) offers a mathematical relationship between the hole-saw ring diameter and the geometric variable X.

Experimental Data Analysis

Results of the measurements of the ring diameters and the related information are presented in the table of Hole-saw Ring Data. The ring pattern starts at $D_p/T = 1.59$ and dispears at about $D_p/T = 15$. The lead targets began showingthe ring pattern at $D_p/T = 1.27$, however the circular pattern has no specific craters that formed the rim of the ring. The rings at this regime have a radically diffused shape. The well defined hole-saw rings started at $D_p/T = 12.50$ and up to $D_p/T = 20.89$ in our observations. For the teflon target, we have employed different impact velocity, from 2.3 km/s to 6.3 km/s, and various target thichness. At low velocity, 2.3 km/s, the ring pattern started to appear at approxmately $D_p/T = 3.90$, and faded away at $D_p/T = 63.5$. The true hole-saw ring has not ever appeared in this impact velocity regime. At 4 km/s velocity, some diffused ring started to show up at $D_p/T = 1.57$, a very nice ring was founded at $D_p/T = 6.35$, and then it dispeared at $D_p/T = 31.75$. The target plates of aluminum alloy 1100 showed the ring pattern from $D_p/T = 1.98$ to $D_p/T = 4.02$.

HOLE-SAW RING DATA
Measured and Computed Values

Target Material	Impact Velocity	D_p (cm)	Shot number	L Standoff	D_p/T	D_t / D_p (cm)	$\xi_{b\ computed}$ (10^{10})	$D_{measured}$ (cm)	ρ_t/ρ_p
Inconel	5.94	0.3175	1109	12.06	4.41	1.61	0.292	2.306	3.24
Inconel	5.76	0.3175	1110	12.06	5.68	1.72	0.227	6.783	3.24
Inconel	5.96	0.3175	1120	12.06	7.82	1.44	0.405	3.691	3.24
Inconel	6.03	0.3175	1119	12.06	9.98	1.34	0.507	3.678	3.24
Lead	6.38	0.3175	65	12.06	12.5	1.57	0.770	5.990	4.11
Lead	6.1	0.3175	66	12.7	20.89	1.51	0.784	2.637	4.11
Teflon	4.03	0.3175	84	13.0	6.35	1.51	1.20	1.201	0.87
Teflon	6.0	0.3175	501	12.46	12.5	1.30	3.44	1.355	0.87
Teflon	6.25	0.3175	34	12.06	1.94	2.68	0.704	6.970	0.87
Teflon	6.31	0.3175	35	12.06	3.97	1.89	1.80	3.115	0.87
Teflon	6.32	0.1000	534	4.76	1.33	3.20	0.436	3.654	0.87
Teflon	6.28	0.1000	547	4.76	3.94	2.16	1.23	3.267	0.87
Teflon	6.25	0.1000	536	4.76	3.94	--	--	2.963	0.87
Al1100	3.85	0.3175	1166	12.06	3.18	1.57	0.853	2.390	1.11
Al1100	5.16	0.3175	1159	12.06	3.11	1.86	1.02	3.826	1.11
Al1100	5.87	0.3175	789	11.35	1.98	2.76	0.456	6.768	1.11
Al1100	5.89	0.3175	793	6.35	1.98	2.78	0.447	4.328	1.11
Al1100	5.86	0.3175	794	6.03	2.40	2.32	0.725	3.624	.11
Al1100	6.03	0.3175	795	6.03	3.01	2.17	0.916	3.010	1.11
Al1100	5.95	0.3175	790	11.35	4.02	2.14	0.943	4.060	1.11
Al1100	5.90	0.3175	740	13.02	4.00	2.11	0.966	3.670	1.11
Al6061	5.92	0.3175	1065	12.06	1.55	2.33	0.743	8.830	1.11
Al6061	6.00	0.3175	1480	12.06	1.98	2.43	0.680	8.951	1.11
Al6061	5.70	0.3175	1483	48.24	1.98	2.43	0.625	32.53	1.11
Al6061	6.06	0.3175	1057	12.06	2.04	2.05	1.10	7.678	1.11
Al6061	5.75	0.3175	1465	12.06	3.13	1.92	1.17	4.399	1.11
Al6061	5.90	0.3175	1479	48.24	3.13	1.90	1.29	22.23	1.11
Al6061	5.86	0.3175	1471	12.06	4.00	1.77	1.49	4.593	1.11
Al6061	5.90	0.3175	1477	48.24	4.00	1.72	1.64	18.31	1.11
Al6061	5.95	0.3175	1484	96.48	4.00	1.80	1.50	35.78	1.11
Al6160	5.65	0.3175	1470	12.06	5.00	1.64	1.66	2.436	1.11
Al6061	5.83	0.3175	1475	48.24	5.00	1.63	1.82	12.41	1.11
Al6061	5.72	0.3175	1469	12.06	5.95	1.52	2.02	1.342	1.11
Al6061	5.20	0.3175	1476	48.24	5.95	1.46	1.83	3.978	1.11
Al6061	6.00	0.3175	1481	12.06	7.81	1.36	2.78	0.929	1.11
Al6061	5.86	0.3175	1482	48.24	7.81	1.33	2.78	4.014	1.11
Al6061	5.91	0.3175	1058	12.06	10.51	1.22	3.25	2.323	1.11

The Aluminum 6061 target has been studied with a systematic change of D_p/T values from 1.55 to 10.51. We tried to control the projectile impact velocity as close as we can to a fixed speed at 6 km/s. The stand-off distance from the target to the witness plate was altered for the different D_p/T values. This procedure helped to uncover the center portion of the ring in much more detail. A major part of the projectile material was melted and the melted material spread on the witness plate produced a web like pattern inside the ring. When the stand-off distance was increased, the web configuration was enhanced and linked the craters on the rim of the hole-saw ring into a circle. The craters inside the ring due to the secondary impact are mostly less than 50 μm for a D_p/T ratio less than 4. When the D_p/T ratio increased the smaller craters disappeared, and the ring diameter decreased as well.

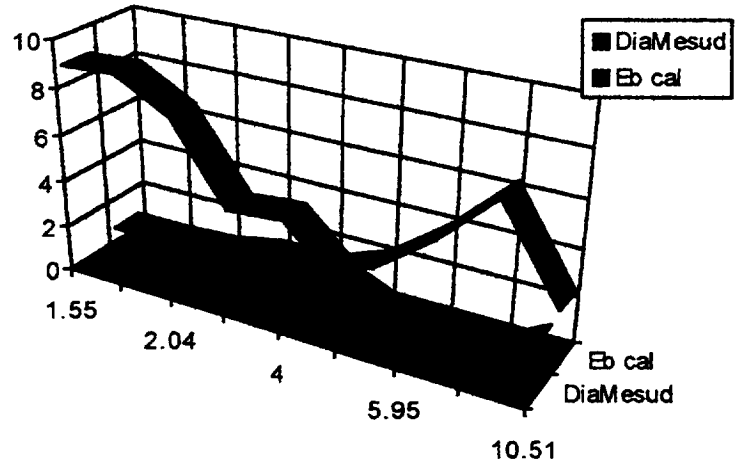

When the D_p/T ratio increases the diameter of the ring decreases and the average energy per unit mass, ξ_b, increases to the maximum value of 3.0×10^{10} erg/gm at about $D_p/T = 8.5$.

For Teflon target, the graph shows the same pattern of the D_p/T - Diameter relationship. The inconel target behaved quite differently.

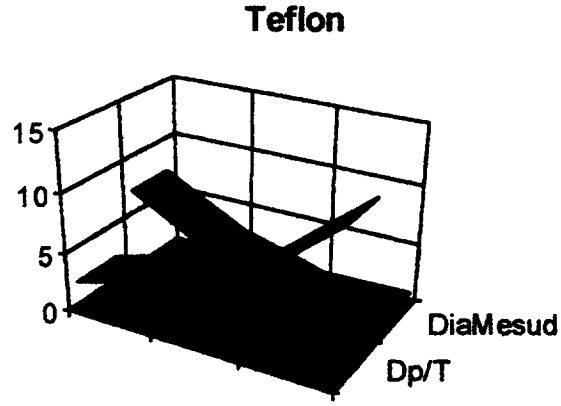

The ring diameter increases with respect to D_p/T ratio increases. After reached a maximum value, it decreased as D_p/T ratio increased.

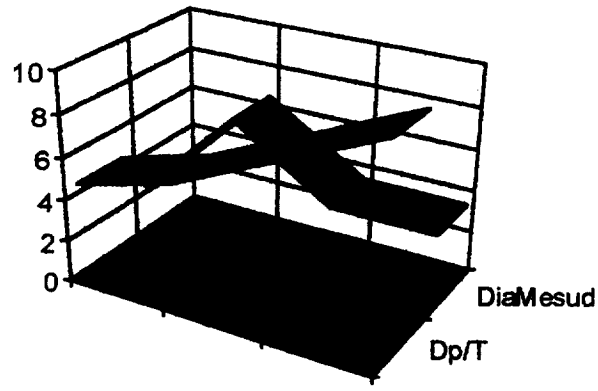

For aluminium 1100 alloy, the diameter of the ring reaches a maxium value at a early stage, then start to drop with respect to the increasing of D_p/T ratio. After reaching a minimum value it started to increase.

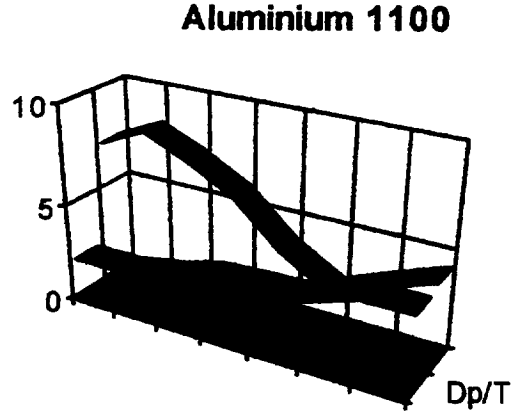

Crater Distribution On The Ring

The craters observed on the hole-saw ring can be classified into four catagories: (1) craters produced by multiple impacts, (2) craters produced by melted projectiles which formed a unusual shape, (3) long string like craters, and (4) single impact created craters. Most the craters that can be seen by the naked eye belong to the fisrt three groups. We have rarely seen the clean, single large craters. The craters in the group (2) caused the most difficulty when we counted the craters and tryed to measure the crater diameter. It was found that all the craters on the ring were produced by the projectiles. The melted projectile material, soda-lime glass, was observed in the craters. At $D_p/T = 4$,

the increase of the stand-off distance shifted the maximum crater occupied area from about 1500 μm craters to a double peak at 1100 μm and 1400 μm craters. The same behavior happened for the D_p/T ratio at 5. The later one shifted from 1200 μm to 1100 μm and 600 μm. The crater distributions are shown in the following charts.

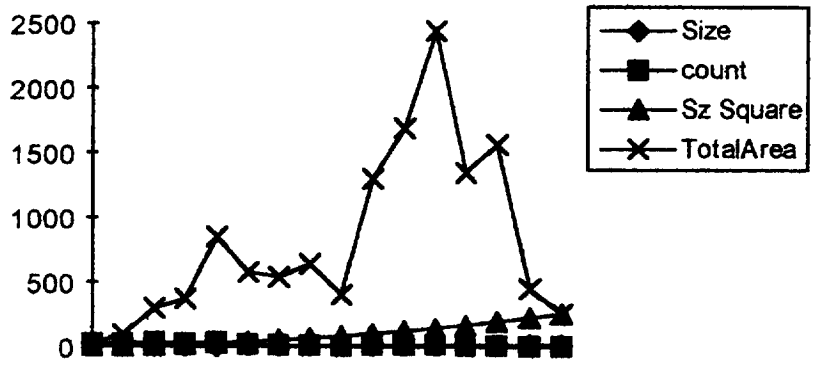

Crater Distribution at Dp/T= 4

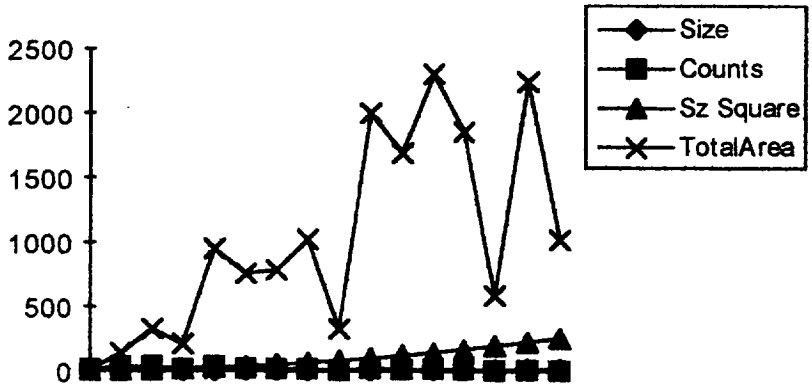

Crater Distribution, Dp/T= 4

The first chart above is the witness plate located at 12.06 cm from the aluminium 6061 target. The second chart is the witness plate located at 28.24 cm from the target plate.

A crater equation by A. Watts (7),

$$\left(\frac{d_c}{d_p}\right) = 1.0857\left(\frac{\rho_p}{\rho_t}\right)^{0.2857}\left(\frac{\rho_t}{Y_t}\right)^{0.2857}\left(\frac{c_t}{c_p}\right)^{0.2857}\frac{u_o^{0.5714}}{\left(1+\left(\frac{\rho_p}{\rho_t}\right)^{1/2}\right)^{0.5714}}, \quad (8)$$

was employed to calculate the fragment mass from the projectile which created the hole-saw ring. The fragment mass distribution isvery similar to the crater distribution. Based

on this calculation, the total mass of the fragments that produced the craters on the ring wasonly a small fractionof the projectile mass.

DISCUSSION AND CONCLUSION

The analytic model was used to calculate the functional relationship between the diameter of hole-saw ring and the D_p/T ratio by assuming that the average breakup energy per unit mass was constant. We selected a known ring diameter value to calculate the ξ_b value, and used the calculated result as a constant to calculate the ring diameter under a different D_p/T ratio in the same impact velocity regime. This procedure shows that the constant ξ_b value is not valid. Our ring diameters calculated by using Eq.(7) differ from the experiment result very much. The melting string and multiple impacted crater could be causes of the deviation.

A wide range of the D_p/T ratio for different target material was observed in our experiment. The ring patterns are observed at D_p/T=1.98 to 4.02 for aluminium 1100 targets, at D_p/T=1.55 to 10.51 for aluminium 6061 targets, at D_p/T=4.41 to 9.98 for inconel targets, at D_p/T=1.33 to 3.94 for teflon targets, and at D_p/T=12.5 to 20.89 for lead targets.

During the ASEE/NASA summer progam period, we have utilized the CTH hydrocode to simulate this complicated phenomenon. The specific ring patterns have not been reproduced successfully. Futher investigation is needed. The special hole-saw ring pattern will serve as a very good boundary condition for the futher understanding of the hypervelocity impact phenomena.

REFERENCES

1. F. Horz, M. Cintala, R. Bernhard and T. See, Dimensionally Scaled Penetration Experiments: Aluminium targets and glass projectiles 50 μm to 3.2 mm in diameter. Int. J. Impact Engng Vol. 15, No. 3, pp. 257-280 (1994).

2. A. J. Stilp, V. Hohler, E. Schneider and K. Weber, Debris cloud expansion studies. Int. J. Impact Engng 10, 543-559 (1990).

3. A. J. Pietkutowsky, A simple dynamic model for the formation of debris cloud. Int. J. Impact Engng 10, 453-472 (1990).

4. X. Weng and C. H. Yew, Hypervelocity impact of two sphere. Int. J. Impact Engng 8, 229-240 (1989).

5. D. E. Grady and S. L. Passmann, stability and fragmentation of ejecta in hypervelocity impact. Int. J. Impact Engng 10, 197-212 (1989).

6. R. J. Lawrence, A simple model for the optimization of stand-off hypervelocity particle shields. Int. J. Impact Engng. Vol. 5, pp. 451-461 (1987).

7. A. Watts, D. Atkinson and S. Rieco, Dimensional scaling for impact cratering and perforation. NASA contractor report, NCR 188259, March 16, 1993.

Sg-34

4172

N95-32427

Baseline Experimental Investigation of an Electrohydrodynamically Assisted Heat Pipe

Final Report
1994 NASA/ASEE Summer Faculty Fellowship Program
Johnson Space Center

Submitted by:
A. B. Duncan[1]

Assistant Professor
University of Illinois at Chicago

NASA/JSC

Directorate: Engineering

Division: Crew and Thermal Systems

Branch: Thermal Systems

JSC Colleague: Kathryn Miller Hurlbert

Date Submitted: August 4, 1994

Contract Number: NGT-44-005-803

Kathryn Miller Hurlbert

Allen B. Duncan

[1]Direct All Correspondence to:
Dr. A. B. Duncan
Department of Mechanical Engineering (M/C 251)
University of Illinois at Chicago
Engineering Research Facility
842 W. Taylor St.
Chicago, IL 60607-7022